

Resolving sugar puckers in RNA excited states exposes slow modes of repuckering dynamics

Mary C. Clay¹, Laura R. Ganser¹, Dawn K. Merriman², and Hashim M. Al-Hashimi *^{1,2}

Supporting Information

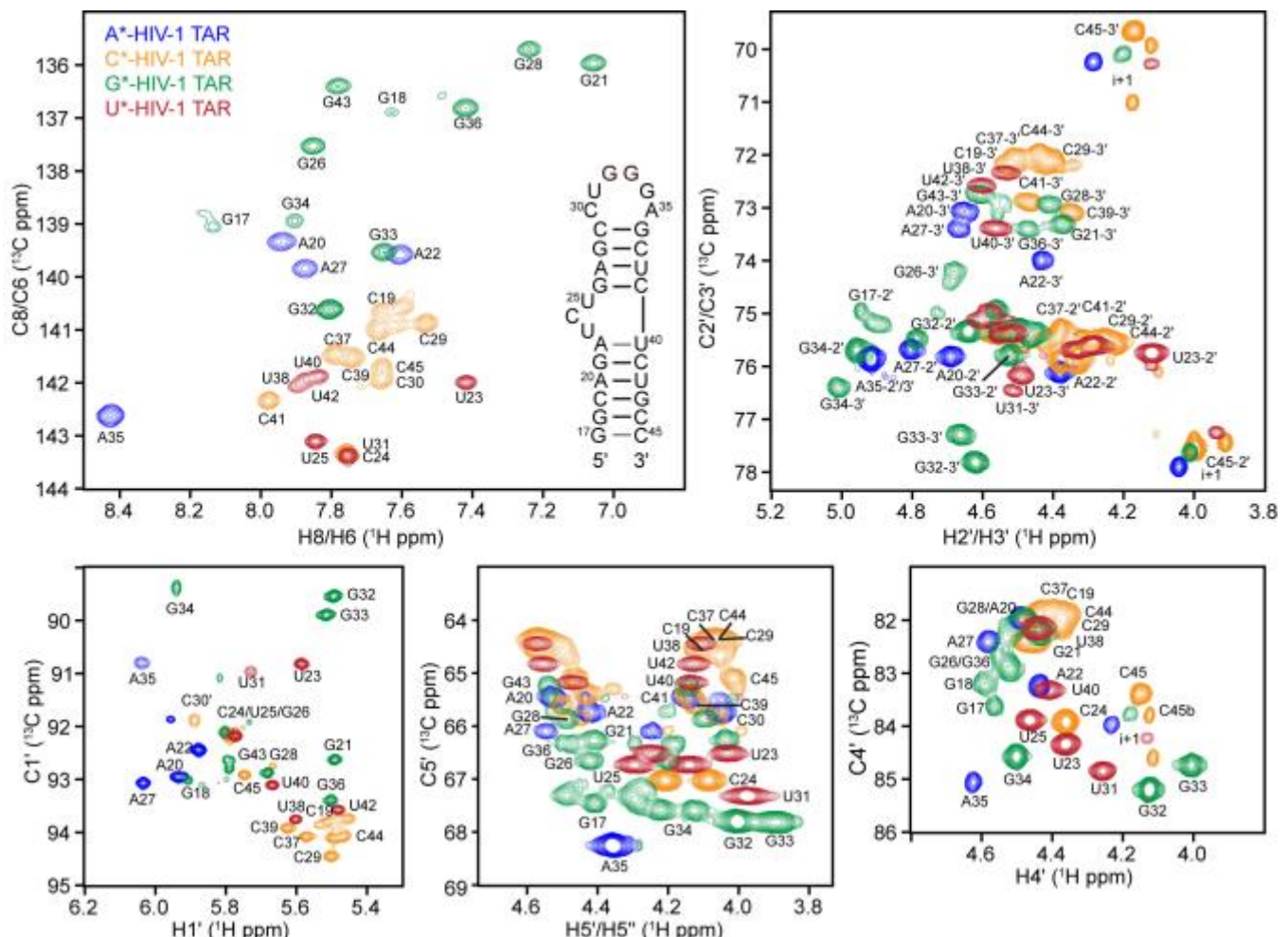


Figure S1. Residue-type $^{13}\text{C}/^{15}\text{N}$ labeling improves NMR spectral resolution for HIV-1 TAR. Shown are overlays of aromatic and sugar 2D HSQC spectra regions for four nucleotide type labeled samples with uniform- $^{13}\text{C},^{15}\text{N}$ labeled adenosine (blue); cytidine (gold); guanosine (green); and uridine (red). Data collected at 600 MHz (^1H frequency spectrometer) and 25 °C. Sample conditions were 1.0–1.4 mM HIV-1-TAR in 15 mM sodium phosphate, 25 mM NaCl, 0.1 mM EDTA, pH 6.4, and 100% D_2O .

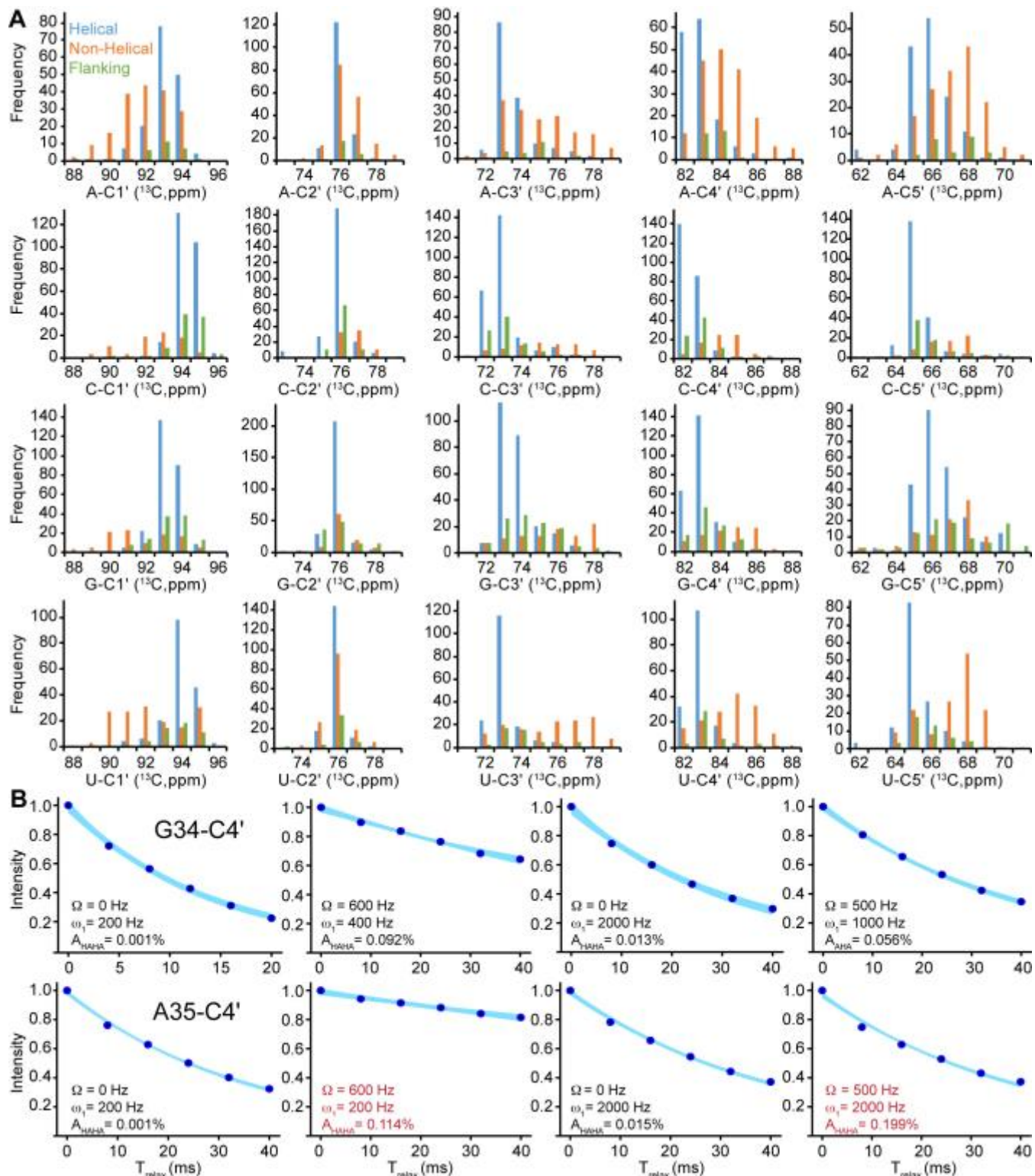


Figure S2. C1' and C4' as R_{1p} RD probes of slow sugar repuckering dynamics. (A) C1', C2', C3', C4', and C5' chemical shifts distributions for different nucleotide types obtained from the BMRB¹ (Table S1) for nucleotides classified as helical (blue), non-helical (orange), or flanking (base paired helical nucleotides next to loops or bulges)(green) based on the available RNA secondary structure. C1' and C4' show a strong dependence on sugar pucker. While C3' and C5' also demonstrate some

dependence on sugar pucker, C3' is not sufficiently resolved to allow for NMR RD studies without the use of site labeling, and the geminal protons on C5' introduce additional relaxation contributions that complicate analysis. C2' does not demonstrate a strong enough dependence on sugar pucker to be a robust reporter, and would also require site labeling to allow for NMR RD measurements. Data shown for adenosine ($N=376$), guanosine ($N=489$), cytidine ($N=434$), and uridine ($N=381$). (B) Example C4' $R_{2,\text{eff}}$ decays showing monoexponential behaviour and no signs of contributions due to C-C interactions. The spin lock field strength (ω_1), offset frequency (Ω), Hartmann-Hahn transfer efficiency (A_{HABA}) are listed in the insets. Data with $A_{\text{HABA}} > 0.1\%$ *i. e.* the off resonance conditions (red insets) shown for A35-C4' would be excluded from further analysis. Data collected on a 600 MHz (^1H frequency) spectrometer at 25 °C with 1.0, 1.3mM HIV-1 TAR in 15 mM sodium phosphate, 25 mM NaCl, 0.1 mM EDTA, pH 6.4 and 100% D₂O.

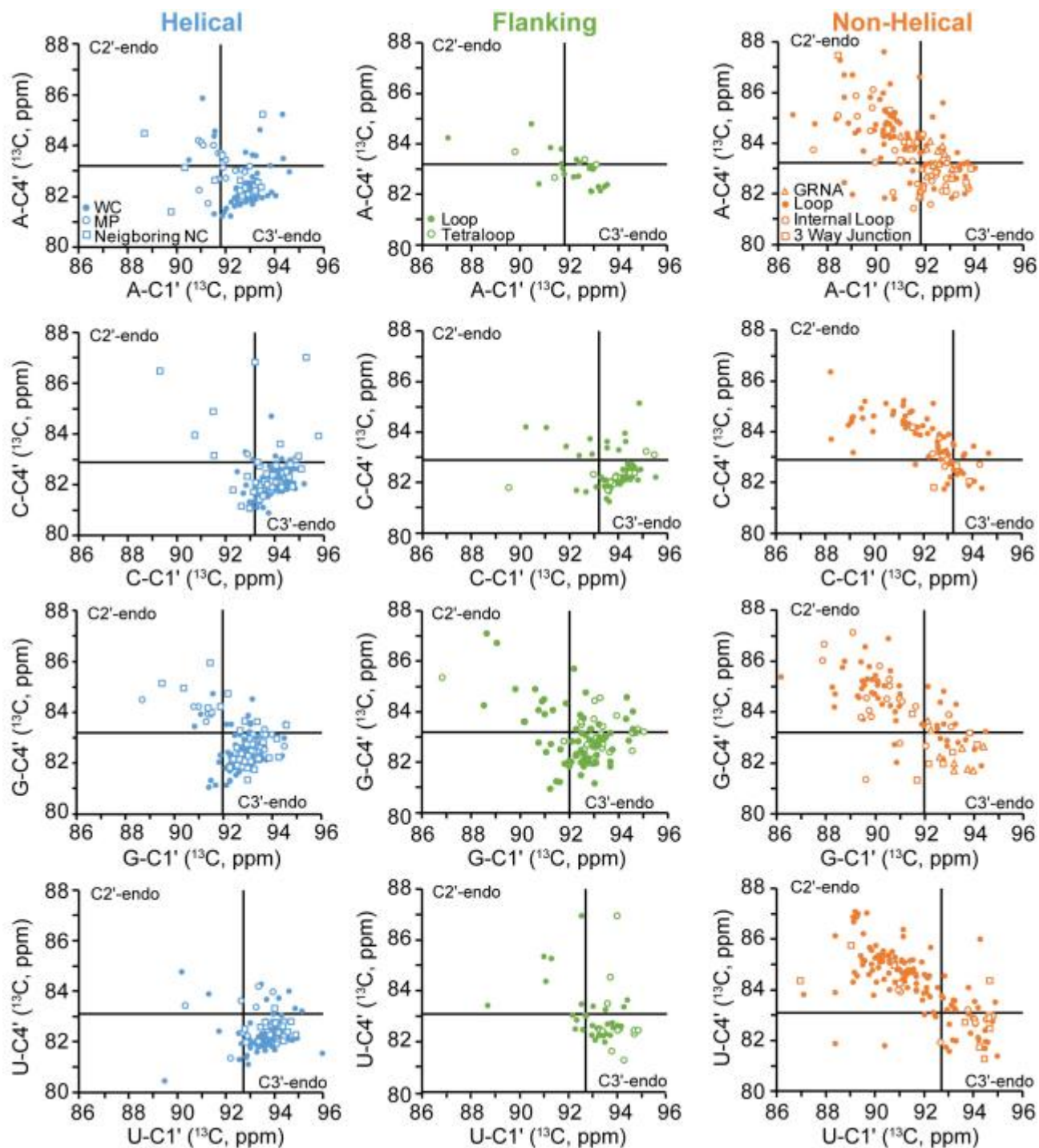


Figure S3. Finer analysis of C1' and C4' chemical shifts and their dependence on RNA structure. C1', C4' correlation plots for individual residue types with solid lines indicating the upper boundaries for the C3'-endo chemical shift region based on the average and standard deviation of observed chemical shifts for helical nucleotides (see Table S2). The location of nucleotides in these four quadrants of the C1', C4' correlation plots indicates the most probable sugar pucker as follows: lower right C3'-endo sugar pucker, upper left dominant C2'-endo pucker (includes C1'-exo), lower left C3'-endo with reduced χ -angle ($-110 \pm 20^\circ$), and upper right C3'-endo with *trans* γ -angle or C2'-endo with *syn* χ -angle. Helical nucleotides were sub-divided into three categories: ● Watson-Crick base pairs, ○ mispairs, and □

Watson-Crick base pairs neighboring non-canonical motifs (i. e. mispairs and pseudoknots). Flanking nucleotides adjacent to tetraloops are shown as ○. Non-helical nucleotides were sub-divided into four categories: ● apical loops and bulges, ○ internal loops, □ three way junctions, and △ nucleotides in GRNA tetraloops. Data shown for adenosine ($N=376$), guanosine ($N=489$), cytidine ($N=434$), and uridine ($N=381$).

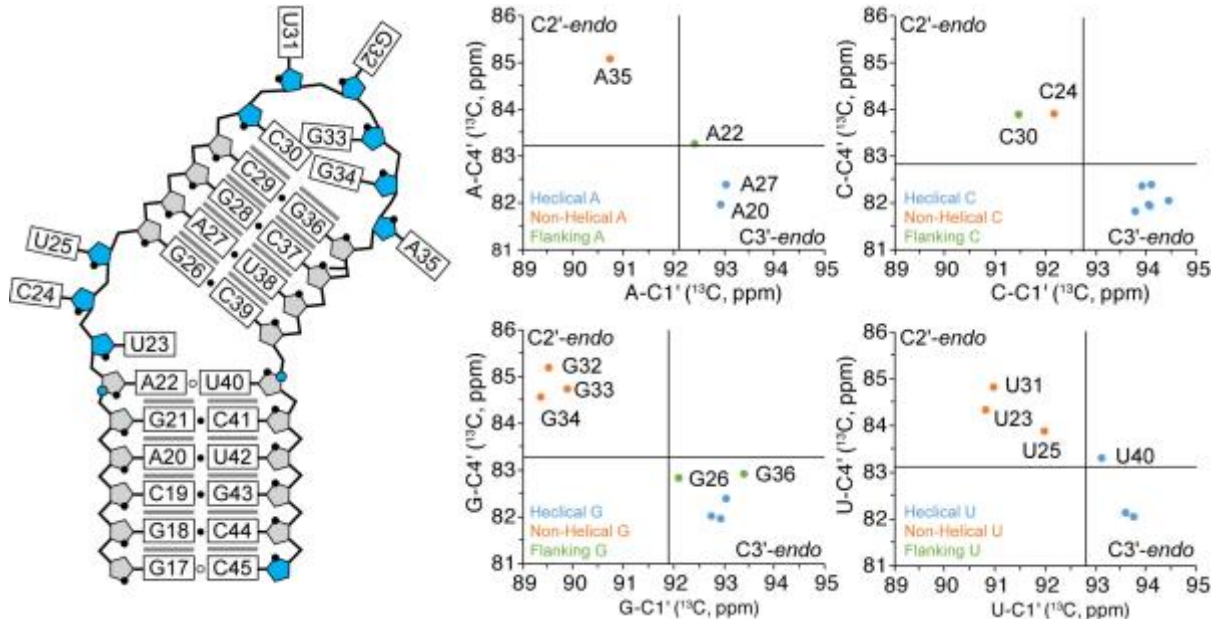


Figure S4. Correlation plot of C1' and C4' chemical shifts for the ground state of HIV-1 TAR. Bulge and apical loop nucleotides fall in the upper left, C2'-endo, quadrant while all helical nucleotides fall within the boundaries of the lower right, C3'-endo, quadrant with the exception of the junctional nucleotides A22 and U40 which have a more downfield shifted C4' chemical shift, possibly due backbone distortions near the bulge. Nucleotides with C2'-endo and C3'-endo sugar pucks are colored blue and gray, respectively. Blue spheres on A22-C4' and U40-C4' indicate deviation of the C4' chemical shifts from the C3'-endo quadrant. Solid lines represent the upper boundaries for the C3'-endo chemical shift region based on the average and standard deviation of observed chemical shifts for helical nucleotides (Table S2). Terminal nucleotides are excluded from the correlation plots.

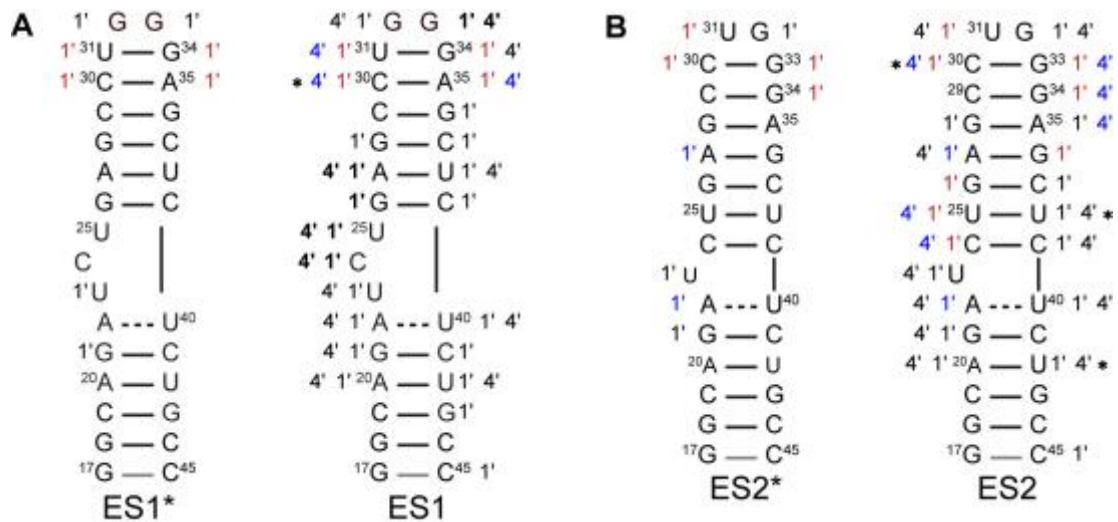


Figure S5. Schematic representation of nucleotides showing C1' and/or C4' RD consistent with (A) ES1 and (B) ES2 exchange. Sites with C1' and/or C4' RD are numbered. Red indicates a downfield shifted ES chemical shift, blue indicates an up-field shifted ES chemical shift, black indicates no detectable RD, and bold indicates absence of μ s ES1 exchange for nucleotides showing ES2 exchange. Asterisks indicates overlapped resonances in the GS for which absence or presence of RD could only be assessed qualitatively. Previously measured RD data (ES1* and ES2*) by Lee *et al.*² and Dethoff *et al.*³ are shown on the left for comparison.

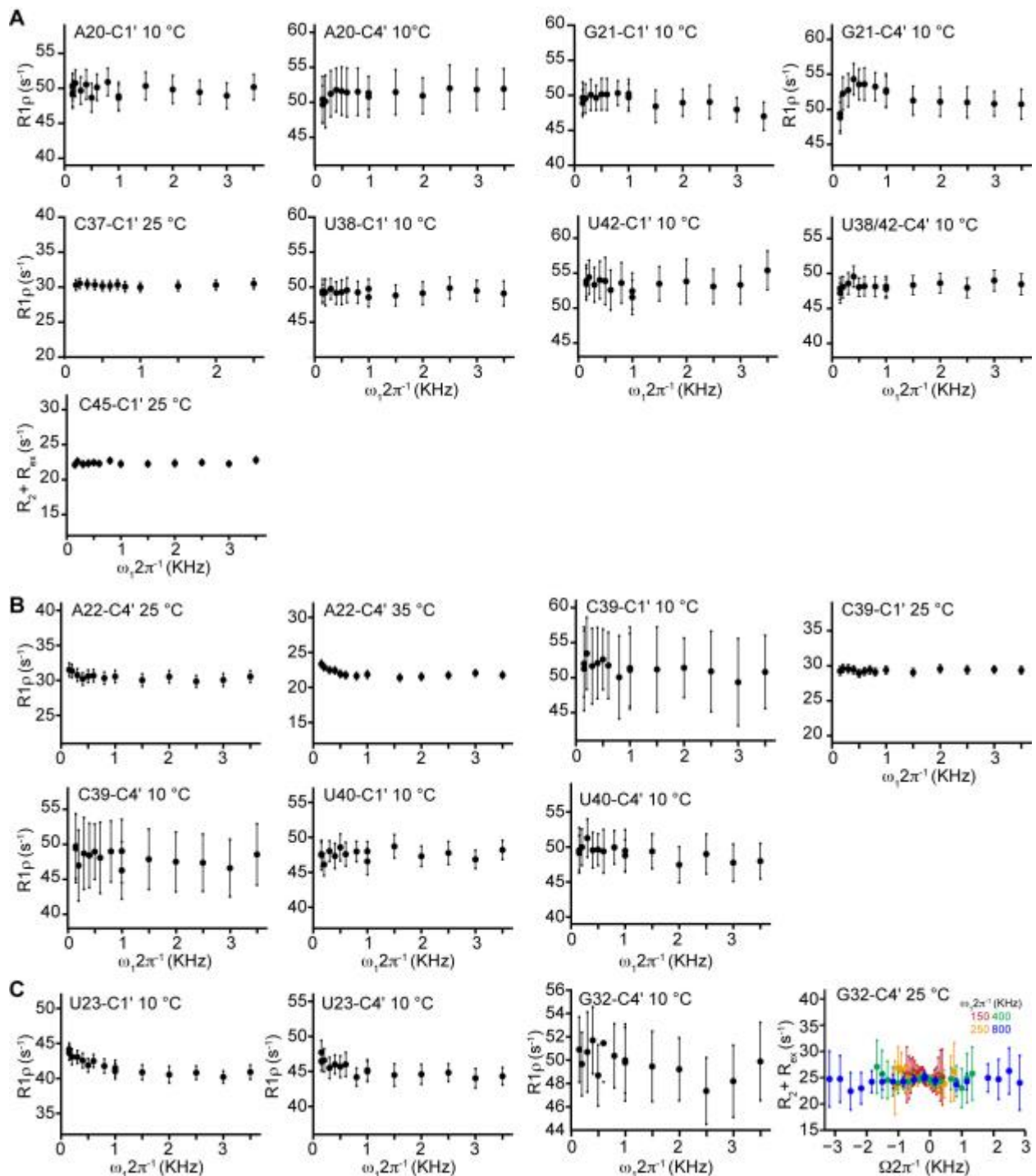


Figure S6. C1' and C4' $R_{1\rho}$ RD profiles showing lack of dispersion for (A) helical (B) junctional and (C) bulge/loop nucleotides that do not undergo changes in secondary structure in either ES1 or ES2. Error bars represent experimental error determined by propagation of error determined by Monte Carlo analysis of monoexponential decay curves and experimental signal to noise. Data was collected on a 600 MHz (^1H frequency) spectrometer with the exception of G21-C1', G21-C4', U38/U40-C4', and G32-C4' which were collected on a 700 MHz (^1H frequency) spectrometer. Sample conditions were 1.0-1.4 mM HIV-1-TAR in 15 mM sodium phosphate, 25 mM NaCl, 0.1 mM EDTA, pH 6.4, and 100% D_2O .

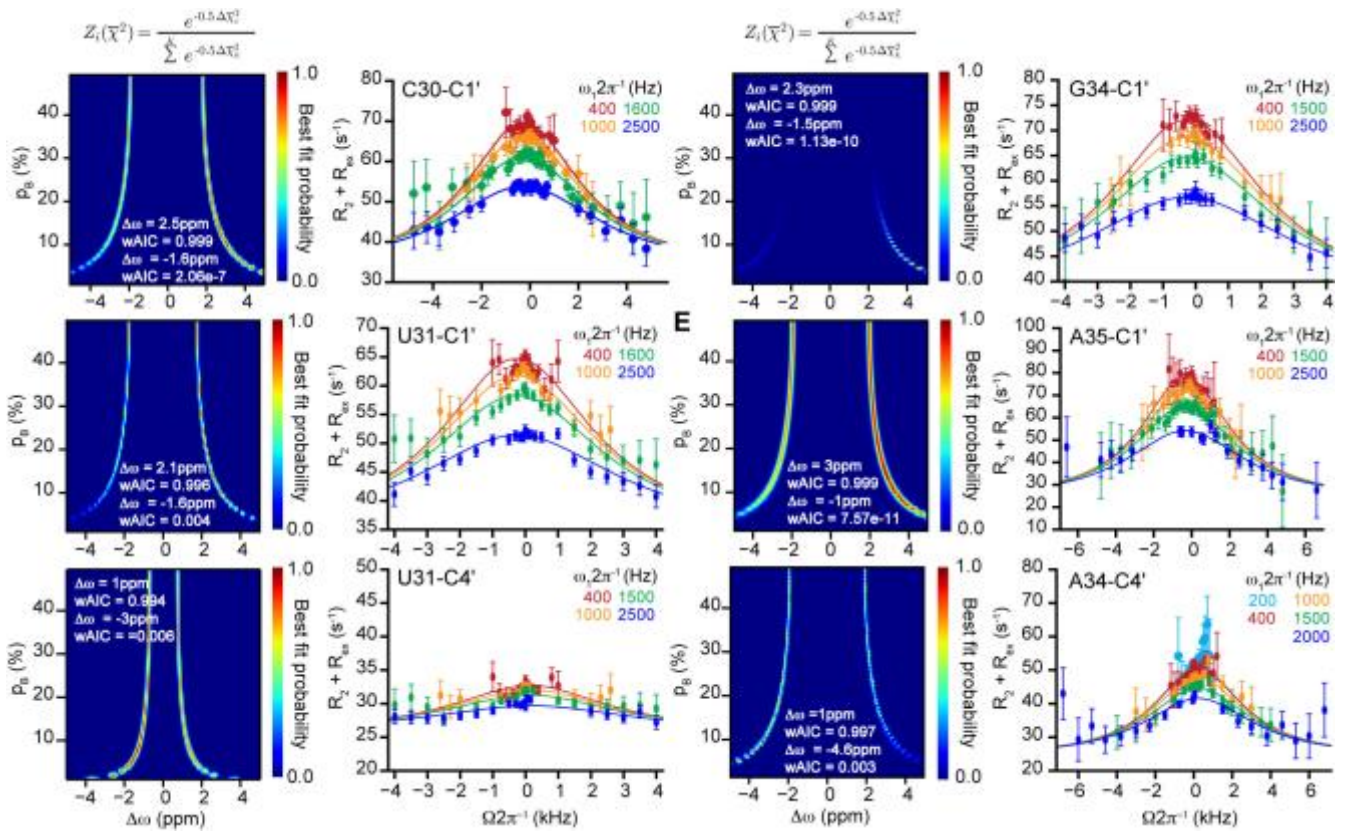


Figure S7. C1' and C4' $R_{1\rho}$ RD profiles for ES1 exchange. Shown to the left of $R_{1\rho}$ profiles are the fit probabilities resulting from a grid search of p_B ($0.0001\% \leq p_B \leq 50\%$) and $\Delta\omega$ (and $-5\text{ppm} \leq \Delta\omega \leq 5\text{ppm}$) values as previously described (5). The χ^2 plots and weighted Akaike information criterion (wAIC) values ($w_AIC = e^{-0.5\Delta AIC_i} / \sum_{k=1}^K e^{-0.5\Delta AIC_k}$ with $\Delta AIC = AIC_i - AIC_{min}$) (6) describes the probability that the fitted sign of $\Delta\omega$ is the correct model as compared to a model in which $\Delta\omega$ has an opposite sign. Error bars on $R_{1\rho}$ profiles represent experimental error determined by propagation of error determined by Monte Carlo analysis of monoexponential decay curves and experimental signal to noise. Data was collected on 600 MHz and (^1H frequency) spectrometer with 1.0-1.4 mM HIV-1-TAR in 15 mM sodium phosphate, 25 mM NaCl, 0.1 mM EDTA, pH 6.4, and 100% D_2O .

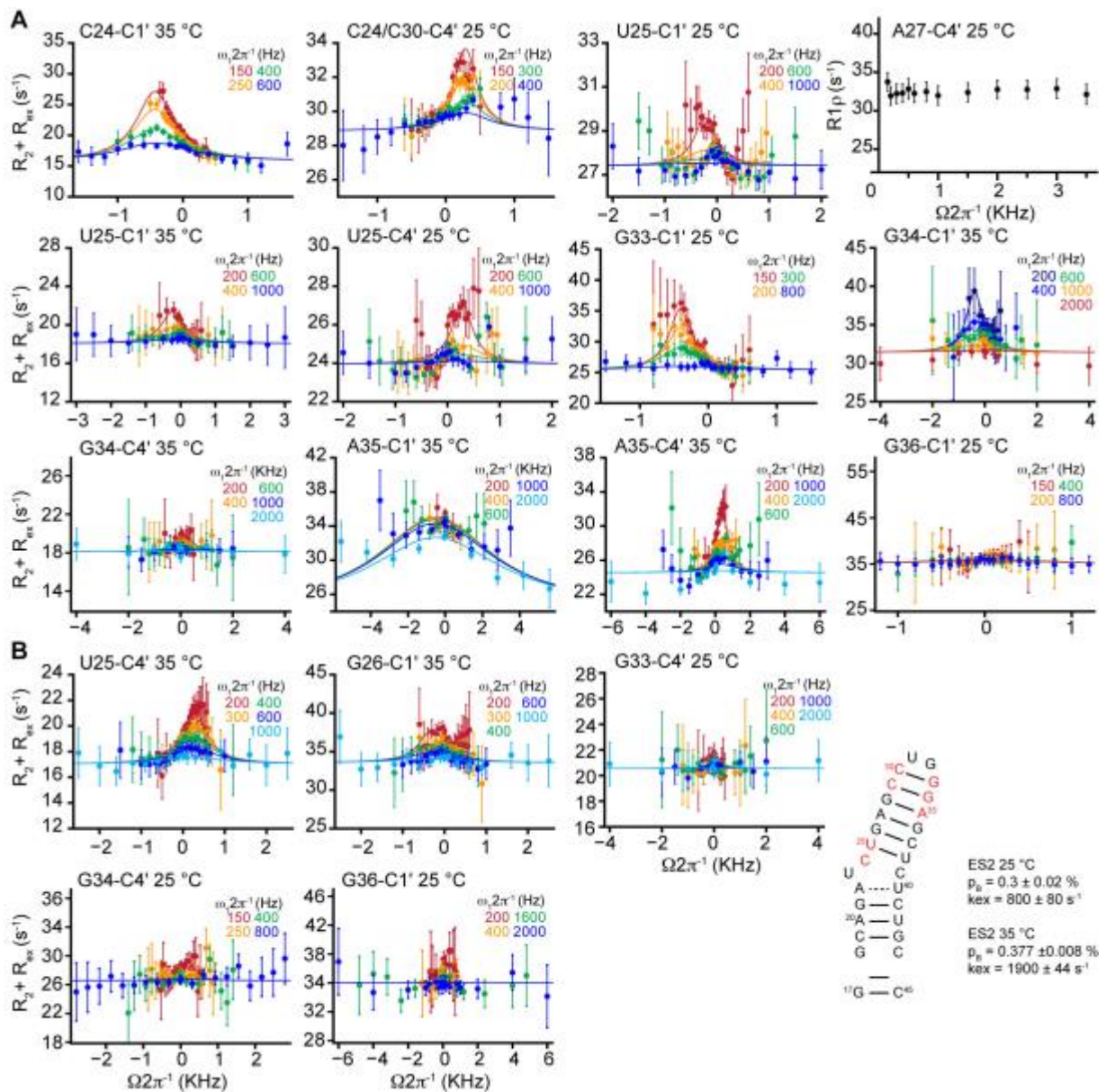


Figure S8. C1' and C4' R_{1p} RD profiles consistent with (A B) ES2 exchange. Error bars represent experimental error determined by propagation of error determined by Monte Carlo analysis of monoexponential decay curves and experimental signal to noise. Data was collected on (A, B) 600 MHz and (C) 700 MHz (^1H frequency) spectrometers with 1.0–1.4 mM HIV-1-TAR in 15 mM sodium phosphate, 25 mM NaCl, 0.1 mM EDTA, pH 6.4, and 100% D_2O .

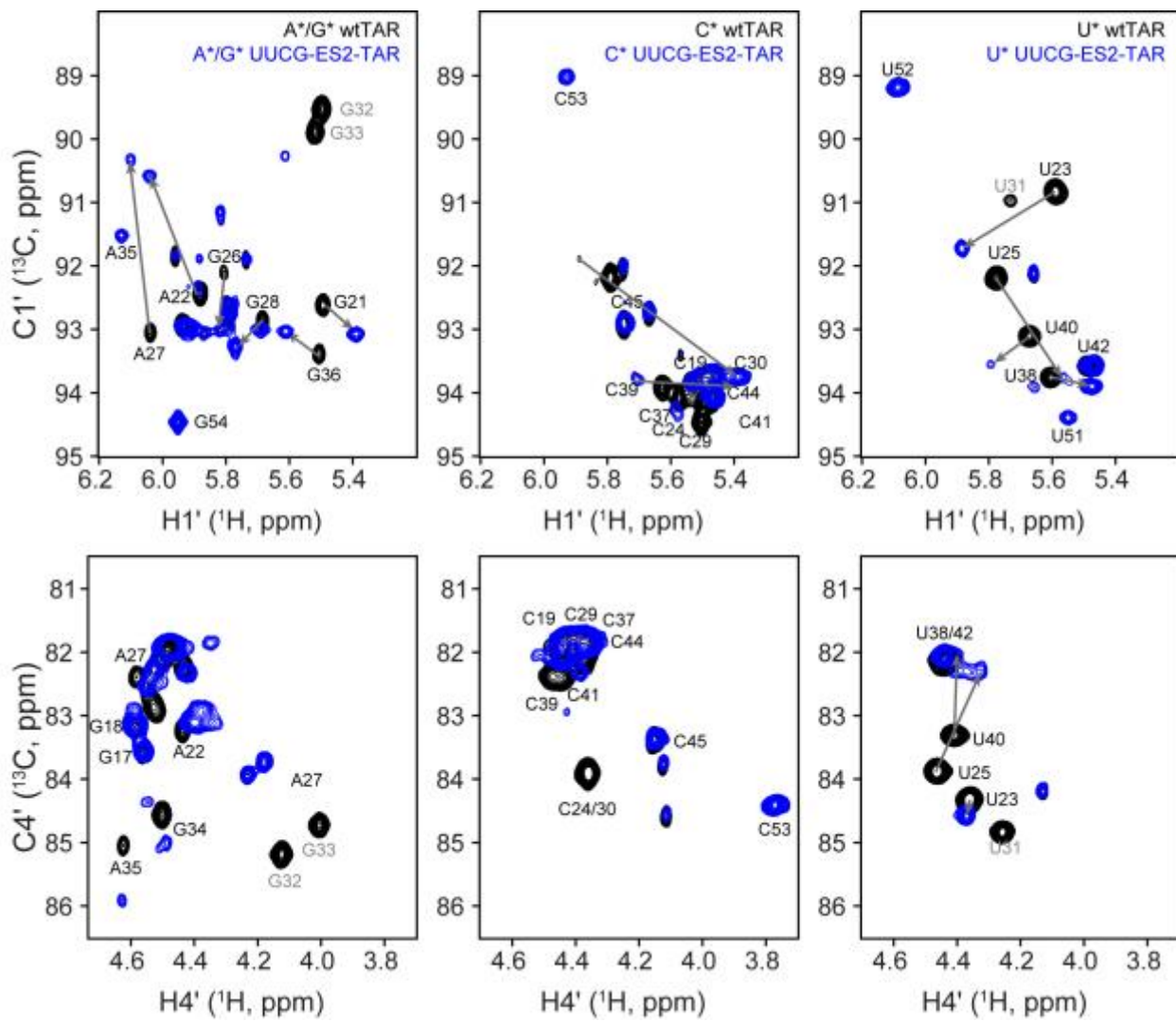


Figure S9. NMR assignments of nucleotide type (A/G, U, and C) $^{13}\text{C}/^{15}\text{N}$ labeled UUCG-ES2-TAR. Shown are overlays of the $\text{H}1'\text{-C}1'$ and $\text{H}4'\text{-C}4'$ regions of CT-HSQC spectra for type labeled samples of HIV-1 TAR (black) and UUCG-ES-TAR (blue). Data collected at 25 °C on a 600 MHz (^1H frequency) spectrometer. Samples were ~ 1mM RNA in 15 mM sodium phosphate, 25 mM NaCl, pH 6.4, and 100% D_2O .

Table S1: Database used to develop chemical shift sugar pucker relationships. Shown are the BMRB entries, PDB codes, primary sequence, and secondary structure denoted using dot bracket notation

BMRB	PDB	Sequence	Secondary Structure
4120	1A60	GGGAGCUCAACUCUCCCCCCC CUUUUCCGAGGGUCAUCGGAA ACCA	(((((.....)))))[[[....(((([]]....))))]....

Table S1: Database used to develop chemical shift sugar pucker relationships. Shown are the BMRB entries, PDB codes, primary sequence, and secondary structure denoted using dot bracket notation

BMRB	PDB	Sequence	Secondary Structure
17572	2LBQ	GGGGACUGUA(¹⁶ A)AUCCCC	(((((.....))))
17941	2LJJ	GGCCUCAGCACUACCCCCAGUGUAGGUC	(((((..((((....))))))))))

18532	2LUN	GGGCAGUGAUGCUCGGCAUAUCAGCCC	(((((((((((....)))))))))))
18549	2LV0	GGGCUAAUGUUGAAAAAUUAGGCC	(((((((((..))))))))
18838	2M12	GGGUGUAUUGGAAAUGAGCACCC	(((((.....))))))
18891 ^b	2M21	GCGAUACACUAUUUAUCGCC	(((((.....))))))
18892	2M22	GGCAGAUCUGUAUUAGAACUGCC	(((((.....)).))))
19018	2M4Q	GGCGUCACACCUUCGGGUGAAGUCGCC	(((((.(((.....))))..))))
19024 ^b	2M4W	GGAAUCGAAAGAUGUCC	(((((.....))).)))
19040	2M58	GGAAGAAAGGGCUUCGGCACUCAAACUACAGA GACGCCAGUCACUCAGAUAUCCUGGU	(((((((((((....))))))))....(((((.....))))).
19634	2MHI	GGAAACGCCGCGGUCAGCUCGGCUGCUGCGAA GAGUUCGUCUCUGUUGUUUCC	(((((..(((.(((.....))))))))..(((.....))))..))))
19692	2MIS	GAGCUGCAGCACGAAAGUGACGGCUC	(((((..(((.....))))))))
19698	2MIY	GCUUGGUGCUUAGCUUUCUUCACCAAGCAUAUU ACACCGGAAUACCGCCAAGGGAGAA	((((((((.....[[[[[[[.]]]]))))....(((((.....))).]]]]].
19873 ^b	2MN0	GGGAGAG(H ² U)GGAACUCCC	(((((.....))))))
25163	2MTJ	GGACCUCCCGUCCUUGGACGGUCGAGCGAAAG CUUGUGAUUGGUCCG	(((((..(((.(((.....))))).(((((.....))))....))))).
25164	2MTK	GGACCUCCCGUCCUUGGACGGUCGAGCGAAAG CUUGUGAUUGGUCCG	(((((..(((.(((.....))))).(((((.....))))....))))).
25603	2N2O	GCAUGUUUUCUGUGAAAACGGUU(((.(((.....))))....
25604	2N2P	GCAUGUUUAGUGUCUAAACGGUU(((.(((.....))))....
25654	2N3Q	GCAGCAGGGAACUCACGCUUGCGUAGAGGCUA AGUGCUCGGCACAGCACAAGCCCGCUGCG	(((((.(((.(((.(((.....))))..))))((..(((((.....))))))).....)))))).
25655	2N3R	GCAGCAGGGAACUCACGCUUGCGUAGAGGCUA AGUGCUCGGCACAGCACAAGCCCGCUGCG	(((((.(((.(((.(((.....))))..))))((..(((((.....))))))).....)))))).
25661	--	GGCAGCCAGAXGAGCACGUUAACGCAAGGCUGU C	(((((.((.....).((.....)).))))))
25826	2N7X	GGUAGUUUUGGCAUGACUCUACC	(((((.(((.....))))))))
26568 ^b	5A17	GACGAUAUCGAGCAUCAAGAGUGAAUAUCGUC	(((((.((((.(((.....))))..))))....))))
26842	--	GGACGACUGAACCGAAAGGUUCUUGGCUGCUU CGGCAGAGGUACGUCC	(((((.(((.(((.....))))....))))....))))

a. Systematic offset of + 10 ppm for C1' and + 7ppm for C2', C3', C4' and C5'

b. Chemical shifts adjusted by adding 2.7 ppm to correct referencing error.⁴

Table S2: Average ^{13}C chemical shifts for nucleotides classified as helical, non-helical, or flanking. Values represent the average and standard deviations over the database shown in Table S1

A-Form Helix (^{13}C , ppm)					
	C1'	C2'	C3'	C4'	C5'
A	92.7 \pm 0.9	75.7 \pm 0.4	73.2 \pm 1.1	82.4 \pm 0.8	65.6 \pm 2.0
G	92.8 \pm 0.8	75.5 \pm 1.1	73.3 \pm 1.1	82.5 \pm 0.8	66.0 \pm 1.4
C	93.9 \pm 0.6	75.5 \pm 1.0	72.7 \pm 1.5	82.1 \pm 0.7	64.8 \pm 1.2
U	93.6 \pm 0.9	75.4 \pm 0.5	72.6 \pm 0.9	82.4 \pm 0.7	64.8 \pm 1.2
Non-Helical (^{13}C , ppm)					
	C1'	C2'	C3'	C4'	C5'
A	91.5 \pm 1.6	76.1 \pm 1.1	74.8 \pm 2.1	83.8 \pm 1.3	66.6 \pm 1.6
G	90.9 \pm 2.1	75.8 \pm 1.2	75.4 \pm 2.1	84.2 \pm 1.3	66.5 \pm 1.8
C	92.0 \pm 1.6	76.3 \pm 0.8	75.2 \pm 2.6	83.6 \pm 1.0	66.4 \pm 1.4
U	91.9 \pm 1.9	75.5 \pm 0.9	75.0 \pm 2.3	84.0 \pm 1.5	66.5 \pm 1.6
Flanking (^{13}C , ppm)					
	C1'	C2'	C3'	C4'	C5'
A	92.2 \pm 1.2	76.0 \pm 1.0	73.7 \pm 1.4	82.8 \pm 0.7	66.5 \pm 1.1
G	92.5 \pm 1.7	75.6 \pm 0.9	74.0 \pm 1.7	83.0 \pm 1.2	66.5 \pm 2.1
C	93.8 \pm 1.1	75.5 \pm 0.8	72.9 \pm 1.3	82.4 \pm 1.4	65.4 \pm 1.5
U	93.0 \pm 1.2	75.6 \pm 0.7	73.5 \pm 1.7	83.0 \pm 1.1	65.3 \pm 1.2

Table S3: Distribution of nucleotides among the four different quadrants of the C1', C4' correlation plots (Figure S2).

Helical	Upper Left	Upper Right	Lower	
			Right	Left
Total	5.0 %	5.6 %	83.4 %	6.0 %
WC	1.4 %	2.8 %	64.9 %	3.7 %
Mispair	1.9 %	0.8 %	6.1 %	0.9 %
NMP	1.7 %	2.0 %	12.4 %	1.4 %
Non-Helical	Upper Left	Upper Right	Lower	
			Right	Left
Total	53.4 %	11.6 %	25.4 %	9.7 %
Internal Loop	6.4 %	1.5 %	4.5 %	2.7 %
Tetraloop	11.4 %	2.7 %	6.3 %	1.3 %
Bulge	4.4 %	0.9 %	0.6 %	0.8 %
Loop	29.7 %	6.1 %	8.1 %	4.2 %
3 Way Junction	1.5 %	0.4 %	5.9 %	0.8 %
Flanking	Upper Left	Upper Right	Lower	
			Right	Left
Total	12.9 %	13.3 %	60.8 %	12.9 %
Tetraloop	2.4 %	4.9 %	13.6 %	2.4 %
Bulge	1.4 %	1.4 %	4.5 %	2.1 %
Internal Loop	1.0 %	0.7 %	10.5 %	1.7 %
3 Way Junction	1.0 %	1.0 %	8.0 %	1.4 %
Loop	5.2 %	4.2 %	22.4 %	4.2 %
Mispair	2.1 %	0.7 %	1.7 %	0.7 %

Table S4: List of spinlock powers and offsets used for $R_{1\rho}$ relaxation dispersion measurements collected on Bruker Avance III 700 MHz and 600 MHz spectrometers.

	Site	On-Resonances Spinlock power (Hz) Off-resonances Spinlock Power (Hz) with{Offsets (Hz)}
25 °C 700 MHz	G21-C1' G21-C4'	150,200,300,400,500,600,800,1000,1500,2000,2500,3000,3500 200 & \pm {100,200,400} 400 & \pm {200,600,800} 600 & \pm {300,600,900} 1000 & \pm {,500,1000,2000} 2000 & \pm {,500,1000,2000,4000}
25 °C 700 MHz	G32-C4' G33-C4'	150,200,250,300,350,400,500,600,700,800, 150 & \pm {10,58,116,174,232,290,348,406,464,522} 250 & \pm {10,97,194,291,388,485,582,679,776,873} 400 & \pm {10,156,312,468,780,936,1092,1248,1404} 800 & \pm {10,311,933,1244,1555,1866,2177,2488,2799}
25 °C 700 MHz	G33-C4'	150,200,250,300,350,400,500,600,700,800, 150 & \pm {10,58,116,174,232,290,348,406,464,522} 250 & \pm {10,97,194,291,388,485,582,679,776,873} 400 & \pm {10,156,312,468,780,936,1092,1248,1404} 800 & \pm {10,311,933,1244,1555,1866,2177,2488,2799}
35 °C 700 MHz	C24-C1'	150,200,250,300,350,400,500,600,700,800,1000,1200,1400,1600,1800, 2000,2500,3500 150 & \pm {10,50,100,125,150,200,250,300,350} 250 & \pm {50,100,150,200,250,300,400,500} 400 & \pm {50,100,200,300,400,500,600,800,1000} 600 & \pm {50,100,200,400,600,800,1000,1200,1400,1600}
35 °C 700 MHz	U25-C4'	150,200,250,300,400,500,600,700,900,1000,1200,1400,1600,2000,2500 200 & {40,120,200,400,600},80,160,240,280,320,360,440,480,520,560,-300 300 & \pm {50,100,200,300,400,500,600},150,250,350,700,900 400 & \pm {50,100,150,200,250,300,350,400,600,1200},500 600 & \pm {75,150,225,300,375,450,550,650,1000,1800},-800,-1500 1000 & \pm {100,300,600,900,1200,1600,2000,2500}
35 °C 700 MHz	G26-C1'	150,200,250,300,400,500,600,700,900,1000,1200,1400,1600,2000,2500 200,& {40,120,200,400,600},80,160,240,280,320,360,440,480,520,560 400,& \pm {50,100,150,200,300,400,600,800},250,350,500,-1000,-1200 600,& \pm {75,150,225,300,375,450,550,650,800,1000,1500,1800} 1000,& \pm {100,300,600,900,1200,1600,2000,2500}
35 °C 700 MHz	G34-C4'	150,200,250,300,400,500,600,700,900,1000,1200,1400,1600,2000,2500 200,& \pm {40,120,200,400,600},80,160,240,280,320,360,440,480,520,- 300,-500 300,& \pm {50,100,200,300,400,500,600},150,250,350,900 400,& \pm {50,100,150,200,300,400,600,800,1200},250,350,500,-1000 600,& \pm {75,150,225,300,375,450,550,650,800,1000,1800},-1500 1000,& \pm {100,300,600,900,1200,1600,2000,2500}

Table S4: List of spinlock powers and offsets used for $R_{1\rho}$ relaxation dispersion measurements collected on Bruker Avance III 700 MHz and 600 MHz spectrometers.

	Site	On-Resonances Spinlock power (Hz) Off-resonances Spinlock Power (Hz) with{Offsets (Hz)}
35 °C 700 MHz	U38-C4' U42-C4'	150,200,250,300,400,500,600,700,900,1000,1200,1400,1600,2000,2500 200 & ± {50,100,200,400,600} 400 & ± {50,100,200,400,1000,1200} 600 & ± {100,400,600,1000,1200,1800} 1000 & ± {100,500,1000,2000,3000} 2500 & ± {100,500,2000,3000,5000}
25 °C 600 MHz	A20-C1' A20-C4'	150,200,300,400,500,600,800,1000,1500,2000,2500,3000,3500 200 & ± {100,200,400} 400 & ± {200,600,800} 600 & ± {300,600,900} 1000 & ± {500,1000,2000} 2000 & ± {500,1000,2000,4000}
25 °C 600 MHz	A22-C4'	150,200,300,400,500,600,800,1000,1500,2000,2500,3000,3500 150 & ± {50,100,200,300,400,500,150,250,350,450,550,600} 200 & ± {50,100,200,300,400,500,600,800},150,250,350,450,550,700 300 & ± {50,100,200,300,400,600,800,1000},250,350,500 400 & ± {50,100,200,300,400,600,800,100,1200}
25 °C 600 MHz	U23-C1'	150,200,300,400,500,600,800,1000,1500,2000,2500,3000,3500 200 & ± {50,100,200,300,400,500,600} 400 & ± {50,100,200,400,600} 600 & ± {50,150,300,450,1500,2000} 1000 & ± {50,100,200,400,600,800,2000,3000}
25 °C 600 MHz	U23-C4'	150,200,300,400,500,600,800,1000,1500,2000,2500,3000,3500 200 & ± {50,100,150,200,250,300,350,400,-500,-600} 400 & ± {50,100,150,200,300,400,800,1000,1200} 600 & ± {50,100,150,200,300,400,900,1000,1200,700} 1000 & ± {50,100,200,300,1000,1500,2000} -400,-600,-800,
25 °C 600 MHz	C24-C4'	150,200,300,400,500,600,700,800,1000,2000,2500,3000,3500 150 & ± {100,150,200,250,300,350,400,500,600},+50 200 & ± {50,100,150,200,250,300,350,400,500},-600 300 & ± {50,100,150,200,250,300,350,400,500},-600 400 & ± {50,100,200,300,400,800,1000,1200,1500},-600
25 °C 600 MHz	U25-C4'	150,200,300,400,500,600,800,1000,1500,2000,2500,3000,3500 200 & ± {50,100,150,200,250,350,400,500,600},300 400 & ± {50,100,200,300,450,550,750,850,950},-650 600 & ± {50,150,300,450,600,750,900,1050},-1300 1000 & ± {50,100,200,300,400,800,1000,1500,2000},-600
25 °C 600 MHz	C30-C1'	200,300,400,500,600,800,1000,1600,2000,2500,3000,3500 400 & ± {50,100,200,300,400,500,600,800,1000} 1000 & ± {50,100,250,500,750,1000,1500,2000,2300,2600} 1600 & ± {50,100,200,300,400,500,800,900,1550,1750,2000,2600,3200,3740,4270,4800} 2500 & ± {50,125,250,375,500,625,700,2000,2500,3125,3750,4250,4800} 3000 & ± {2400,3000,4000,8000,9000}

Table S4: List of spinlock powers and offsets used for $R_{1\rho}$ relaxation dispersion measurements collected on Bruker Avance III 700 MHz and 600 MHz spectrometers.

	Site	On-Resonances Spinlock power (Hz) Off-resonances Spinlock Power (Hz) with(Offsets (Hz))
25 °C 600 MHz	U31-C4'	200,300,400,500,600,800,1000,1500,2000,2500,3000,3500 400 & $\pm \{50,100,200,300,400,800,1000\}$ 1000 & $\pm \{50,100,250,1500,2000,2300,2600\}, -500, -750$ 1500 & $\pm \{50,250,1000,1500,2000,2500,3000,3500,4000\}, -500, -750$ 2500 & $\pm \{50,150,1000,1500,2000,2500,3000,3500,4000\}, -300, -500$
25 °C 600 MHz	G33-C1'	200,300,400,500,600,800,1000,1600,2000,2500,3000,3500 150 & $\pm \{50,100,150,200,250,300,350,400,500,600\}, -700, -800$ 200 & $\pm \{100,150,200,250,300,350,400,500,600\}, -700, -800$ 300 & $\pm \{100,150,200,250,300,350,400,500,600\}, -700, -800$ 800 & $\pm \{100,200,300,400,600,800,1000,1200,1500\}$
25 °C 600 MHz	A20-C1' A20-C4'	150,200,300,400,500,600,800,1000,1500,2000,2500,3000,3500 200 & $\pm \{100,200,400\}$ 400 & $\pm \{200,600,800\}$ 600 & $\pm \{300,600,900\}$ 1000 & $\pm \{500,1000,2000\}$ 2000 & $\pm \{500,1000,2000,4000\}$
25 °C 600 MHz	A22-C4'	150,200,300,400,500,600,800,1000,1500,2000,2500,3000,3500 150 & $\pm \{50,100,200,300,400,500,150,250,350,450,550,600\}$ 200 & $\pm \{50,100,200,300,400,500,600,800\}, 150,250,350,450,550,700$ 300 & $\pm \{50,100,200,300,400,600,800,1000\}, 250,350,500$ 400 & $\pm \{50,100,200,300,400,600,800,100,1200\}$
25 °C 600 MHz	U23-C1'	150,200,300,400,500,600,800,1000,1500,2000,2500,3000,3500 200 & $\pm \{50,100,200,300,400,500,600\}$ 400 & $\pm \{50,100,200,400,600\}$ 600 & $\pm \{50,150,300,450,1500,2000\}$ 1000 & $\pm \{50,100,200,400,600,800,2000,3000\}$
25 °C 600 MHz	U23-C4'	150,200,300,400,500,600,800,1000,1500,2000,2500,3000,3500 200 & $\pm \{50,100,150,200,250,300,350,400, -500, -600\}$ 400 & $\pm \{50,100,150,200,300,400,800,1000,1200\}$ 600 & $\pm \{50,100,150,200,300,400,900,1000,1200,700\}$ 1000 & $\pm \{50,100,200,300,1000,1500,2000\} -400, -600, -800,$
25 °C 600 MHz	C24-C4'	150,200,300,400,500,600,700,800,1000,2000,2500,3000,3500 150 & $\pm \{100,150,200,250,300,350,400,500,600\}, +50$ 200 & $\pm \{50,100,150,200,250,300,350,400,500\}, -600$ 300 & $\pm \{50,100,150,200,250,300,350,400,500\}, -600$ 400 & $\pm \{50,100,200,300,400,800,1000,1200,1500\}, -600$
25 °C 600 MHz	U25-C4'	150,200,300,400,500,600,800,1000,1500,2000,2500,3000,3500 200 & $\pm \{50,100,150,200,250,350,400,500,600\}, 300$ 400 & $\pm \{50,100,200,300,450,550,750,850,950\}, -650$ 600 & $\pm \{50,150,300,450,600,750,900,1050\}, -1300$ 1000 & $\pm \{50,100,200,300,400,800,1000,1500,2000\}, -600$

Table S4: List of spinlock powers and offsets used for $R_{1\rho}$ relaxation dispersion measurements collected on Bruker Avance III 700 MHz and 600 MHz spectrometers.

	Site	On-Resonances Spinlock power (Hz) Off-resonances Spinlock Power (Hz) with(Offsets (Hz))
25 °C 600 MHz	C30-C1'	200,300,400,500,600,800,1000,1600,2000,2500,3000,3500 400 & $\pm \{50,100,200,300,400,500,600,800,1000\}$ 1000 & $\pm \{50,100,250,500,750,1000,1500,2000,2300,2600\}$ 1600 & $\pm \{50,100,200,300,400,500,800,900,1550,1750,2000,2600,3200,3740,4270,4800\}$ 2500 & $\pm \{50,125,250,375,500,625,700,2000,2500,3125,3750,4250,4800\}$ 3000 & $\pm \{2400,3000,4000,8000,9000\}$
25 °C 600 MHz	U31-C4'	200,300,400,500,600,800,1000,1500,2000,2500,3000,3500 400 & $\pm \{50,100,200,300,400,800,1000\}$ 1000 & $\pm \{50,100,250,1500,2000,2300,2600\}, -500, -750$ 1500 & $\pm \{50,250,1000,1500,2000,2500,3000,3500,4000\}, -500, -750$ 2500 & $\pm \{50,150,1000,1500,2000,2500,3000,3500,4000\}, -300, -500$
25 °C 600 MHz	G33-C1'	200,300,400,500,600,800,1000,1600,2000,2500,3000,3500 150 & $\pm \{50,100,150,200,250,300,350,400,500,600\}, -700, -800$ 200 & $\pm \{100,150,200,250,300,350,400,500,600\}, -700, -800$ 300 & $\pm \{100,150,200,250,300,350,400,500,600\}, -700, -800$ 800 & $\pm \{100,200,300,400,600,800,1000,1200,1500\}$
35 °C 600 MHz	A35-C1'	150,200,300,400,500,600,800,1000,1600,2000,2500,3000,3500 200 & $\pm \{50,140,280,420\}$ 400 & $\pm \{50,280,560,840\}$ 600 & $\pm \{50,420,840,1260,1680,2100\}$ 1000 & $\pm \{50,700,1400,2100,2800,3500\}$ 2000 & $\pm \{50,1400,2800,4200,5600,7000\}$
35 °C 600 MHz	A35-C4'	150,200,300,400,500,600,800,1000,1500,2000,2500,3000,3500 200 & $\pm \{50,100,200,400,600\}, 150,250,300,350,450,500$ 400 & $\pm \{50,100,200,400,600,800,1000,1200\}, 150,250,300,350,450,500$ 600 & $\pm \{50,100,200,400,500,600,800,1000,1200,1400,2000,2500\}, 300$ 1000 & $\pm \{50,100,250,500,1000,1500,2000,2500,3000\}$ 2000 & $\pm \{50,500,1000,2000,4000,6000,7600\}$

Table S5: Exchange parameters obtained from globally fitting C1' and C4' sugar RD data measured in HIV-1 TAR

Res	Temp (°C)	$\Delta\omega_B$ (ppm)	p_B (%)	k_{exAB} (s ⁻¹)	R_1 (s ⁻¹)	R_2 (s ⁻¹)	AIC	BIC
C30-C1'	25	2.53 ± 0.11	13.8 ± 1.4	18000 ± 400	1.05 ± 0.16	32.47 ± 0.87	-339	-202
U31-C1'		2.32 ± 0.10			1.09 ± 0.11	33.46 ± 0.71		
U31-C4'		-1.00 ± 0.07			1.69 ± 0.08	26.10 ± 0.39		
G34-C1'		2.49 ± 0.11			1.56 ± 0.17	36.06 ± 0.93		
A35-C1'		3.09 ± 0.14			2.13 ± 0.29	2.24 ± 1.56		
A35-C4'		-2.14 ± 0.10			1.84 ± 0.10	23.45 ± 0.82		
C24/30-C4'	25	-1.88 ± 0.06	0.30 ± 0.02	800 ± 80	2.47 ± 0.04	28.85 ± 0.06	-4.6	156
U25-C1'		1.53 ± 0.09			1.43 ± 0.05	27.41 ± 0.06		
U25-C4'		-1.83 ± 0.11			1.85 ± 0.06	23.94 ± 0.07		
G33-C1'		2.69 ± 0.16			1.65 ± 0.08	25.39 ± 0.11		
G34-C4'		-1.21 ± 0.12			1.25 ± 0.06	26.55 ± 0.13		
A35-C4'		-2.32 ± 0.41			1.86 ± 0.13	23.27 ± 0.81		
G36-C1'		1.24 ± 0.27			0.87 ± 0.12	36.02 ± 0.19		
A35-C4'		-2.51 ± 0.45			1.88 ± 0.14	20.29 ± 2.54		
C24-C1'	35	2.43 ± 0.06	0.377 ± 0.008	1933 ± 44	1.98 ± 0.05	15.78 ± 0.07	-425	-272
U25-C1'		1.64 ± 0.08			1.98 ± 0.05	18.06 ± 0.09		
U25-C4'		-1.56 ± 0.04			1.88 ± 0.05	17.01 ± 0.08		
G26-C1'		1.62 ± 0.08			1.20 ± 0.07	33.5 ± 0.2		
G33-C4'		-0.6 ± 0.2			2.21 ± 0.07	20.55 ± 0.10		
G34-C1'		2.6 ± 0.2			1.8 ± 0.1	31.4 ± 0.2		
G34-C4'		-1.12 ± 0.09			2.24 ± 0.07	18.14 ± 0.10		
A35-C4'		-2.52 ± 0.05			1.98 ± 0.04	24.54 ± 0.06		

References:

1. Ulrich,E.L., Akutsu,H., Doreleijers,J.F., Harano,Y., Ioannidis,Y.E., Lin,J., Livny,M., Mading,S., Maziuk,D., Miller,Z., et al. (2008) BioMagResBank. *Nucleic Acids Res.*, 36, 402–408.
2. Lee,J., Dethoff,E. a and Al-Hashimi,H.M. (2014) Invisible RNA state dynamically couples distant motifs. *Proc. Natl. Acad. Sci. U. S. A.*, 111, 9485–90.
3. Dethoff,E.A., Petzold,K., Chugh,J., Casiano-Negroni,A. and Al-Hashimi,H.M. (2012) Visualizing transient low-populated structures of RNA. *Nature*, 491, 724–8.
4. Aeschbacher,T., Schubert,M. and Allain,F.H.T. (2012) A procedure to validate and correct the ^{13}C chemical shift calibration of RNA datasets. *J. Biomol. NMR*, 52, 179–190.
5. Bothe,J.R., Stein,Z.W. and Al-Hashimi,H.M. (2014) Evaluating the uncertainty in exchange parameters determined from off-resonance R1rho; relaxation dispersion for systems in fast exchange. *J. Magn. Reson.*, **244**, 18–29.
6. Wagenmakers,E.-J. and Farrell,S. (2004) AIC model selection using Akaike weights. *Psychon. Bull. Rev.*, **11**, 192–196.